

# Image Identification and Error Correction Method for Test Report Based on Deep Reinforcement Learning and IoT Platform in Smart Laboratory

XiaoJun Li, State Grid Sichuan Electric Power Corporation Metering Center, China\*  
PeiDong He, State Grid Sichuan Electric Power Corporation Metering Center, China  
WenQi Shen, State Grid Sichuan Electric Power Corporation Metering Center, China  
KeLi Liu, State Grid Sichuan Electric Power Corporation Metering Center, China  
ShuYu Deng, State Grid Sichuan Electric Power Corporation Metering Center, China  
LI Xiao, State Grid Sichuan Electric Power Corporation Metering Center, China

## ABSTRACT

In order to solve the problems that most models are complex, time-consuming, and have difficulty in identifying image errors, an image identification and error correction method of test report based on deep reinforcement learning and the internet of things platform in the smart lab was proposed. Firstly, a smart lab architecture was designed based on the internet of things platform, achieving efficient operation of the laboratory through cloud edge collaboration. Then, the depth separable convolution improved convolutional neural network is used to extract image features, and the features are input into bidirectional recurrent neural networks (BiLSTM) for analysis to complete image recognition. Finally, the ICNN-BiLSTM model is used as the agent of reinforcement learning, and image error correction is completed by identifying the distance between the image and the key points of the reference image. Based on the Python platform, the proposed method was experimentally demonstrated, and the results showed that its average error correction accuracy reached 96.75%, with a processing time of 15.37s.

## KEYWORDS

deep reinforcement learning, ICNN-BiLSTM model, image error correction, image recognition, Internet of Things platform, smart laboratory, test report

## 1. INTRODUCTION

With the continuous development of computer technology and communication technology, State Grid Corporation of China proposed the development strategy of “International Leading Energy Internet Enterprise” to promote the intelligent upgrading of power grid business and realize the digital transformation of marketing measurement system (Ersheng et al., 2020). Currently in traditional

DOI: 10.4018/IJITSA.337797

\*Corresponding Author

This article published as an Open Access article distributed under the terms of the Creative Commons Attribution License (<http://creativecommons.org/licenses/by/4.0/>) which permits unrestricted use, distribution, and production in any medium, provided the author of the original work and original publication source are properly credited.

laboratories, the information between various devices is isolated, lacking effective connections and with a high workload of data maintenance; the experimental equipment lacks necessary identity verification information, and the usage and location information of the equipment cannot be mastered; there is also a lack of linkage between experimental personnel and equipment (Fernandes et al., 2018; Sardjono, 2021). The traditional laboratory has reached the stage where it must be upgraded and transformed. It is needed to build an interconnected intelligent laboratory integrated with the management platform using advanced technologies such as big data and microservices in the background of ubiquitous power from Internet of Things (IoT) and centering on communication management, data storage, computing analysis, business applications, data sharing, etc. (Giacomo et al., 2023).

Although laboratories in China have developed rapidly, various types of power grid equipment are also constantly increasing, and different equipment manufacturers are not the same. The interface types and data transmission protocols of the equipment are not the same, rendering it difficult to automate equipment inspections. At the same time, the laboratory testing process is very cumbersome, and the obtained experiments and test results cannot be automatically processed, requiring a large amount of manual collection, analysis, and uploading, resulting in very low efficiency. Therefore, there is an urgent need for intelligent and information-based management methods to achieve efficient analysis and to process equipment testing information.

The image recognition and error correction for testing reports of power grid equipment is a key business capability of the laboratory. At present, traditional image recognition methods include feature detection method, support vector machine (SVM) machine learning recognition method, BP neural network method, etc. However, these methods have a cumbersome processing process, low accuracy, and are not suitable for the recognition of test report images for power grid equipment (Lu et al., 2022; Masayuki et al., 2022). Recently, scholars are gradually increasing research on the direct use of deep reinforcement learning (DRL) for classification, but the classification effect is greatly influenced by the selection of agents. Meanwhile, present research on image error correction is mostly based on error correction output codes; however, redundant information is added in this approach, causing the waste of computing resources (Najib et al., 2022). As a result, drawing on the increasingly mature deep learning network and IoT technology, this paper proposes an image identification and error correction method for test report based on DRL and IoT platform in the smart laboratory. Compared with traditional methods, the innovation of the proposed method lies in:

- 1) In order to improve the accuracy of image recognition, the proposed method adopts deep separable convolution to simplify the structure of convolutional neural networks (CNN) and combines it with bidirectional recurrent neural networks to ensure the network's fast feature extraction.
- 2) Due to the possibility of dimensionality disasters in traditional Q-learning algorithms, the proposed method uses the ICNN-BiLSTM model as an intelligent agent for reinforcement learning to make action decisions, further ensuring the reliability of error correction results.

## 2. RELATED RESEARCH

Both domestic and international scholars have conducted research on image recognition from the perspectives of feature extraction and machine learning, and a series of research results have been obtained. When the computer's computing power is limited, researchers often manually extracted image features first and then performed image recognition (Guoming & Qinghua 2022). In image feature extraction, algorithms such as local binary patterns (LBP), histogram of oriented gradient (HOG), and Haar-like feature (HL) are widely used. As proposed by Xinrong et al (2022), a multi exposure image fusion technique based on multi-scale block LBP operator is proposed, which constructs an initial weight map by calculating the texture changes, brightness, and spatial consistency weights of the image and uses a multi-resolution method for image recognition. Song (2021) adopts the color threshold segmentation method and morphological processing to reduce interference in the

background area and to enhance the contour of the marker area. And the HOG method is used to collect the gradient or edge direction histogram of each pixel in the residential unit to complete the recognition of traffic signs. Chen and Wang (2020) uses edge detection methods to separate the target vehicle image from the background and binarizes the image. At the same time, Bayesian classifiers are used to achieve intelligent recognition of vehicle models based on different feature value categories. Although the above methods can achieve the extraction and recognition of image features, there are strict requirements for the shooting conditions of the original image. If the obtained image has uneven lighting, it will greatly affect the recognition results. In addition, the feature algorithm itself also has some drawbacks, for instance, the HOG algorithm itself does not have scale invariance.

In recent years, with the enhancement of computer's computing power and neural network models have transformed from theory to reality. This deep learning model can discover complex structures in big data and plays a crucial role in speech recognition, visual target recognition, target detection, etc. (Chavarkar, 2023). Dongxing et al. (2022) proposes an image recognition method based on BP neural network and ASGS CWOA (adaptive shrinking grid search chaos wolf optimization algorithm), in which ASGS CWOA is used to optimize BP neural network parameters and to identify images. This method has a simple structure and low computational complexity, but it does not perform well in image recognition in complex backgrounds. Zhiyu et al. (2020) focuses on the improvement and application history of CNN, starting from its own structure and applications in various fields, summarizes the improvement and optimization directions of CNN in recent years, and shows many research results in the field of image recognition. Jianguo et al. (2022) proposes a student human motion feature image recognition based on graph neural networks, which combines image recognition technology with graph neural network management to achieve object detection and tracking. However, this method did not consider the impact of environmental factors, and the recognition effect needs to be improved. Shintaro et al. (2023) creates an image recognition dataset and uses YOLOv4 and YOLOv7 for image recognition. Although YOLOv4 network has a good analytical ability, it has many model parameters and low recognition efficiency. Zhenyu et al. (2021) utilizes attention convolutional neural networks (ACNN) to extract features from query images and uses a feature matching classifier (FMC) to calculate the similarity score between the feature map and the prototype, thus, completing the image recognition. This method combines ACNN and FMC to achieve recognition accuracy for static images, but its recognition performance needs to be further improved for image recognition in dynamic environments. Lifeng et al. (2022) proposes an image recognition method based on DenseNet and Deep Cone Residual Network (DPRN), in which the parallel feature extraction is performed using an extended convolutional module and is fused with DenseNet to construct an image recognition model. This model overcomes the problems of model complexity and large memory usage in DenseNet and can accurately recognize images, but it is difficult to identify errors in images. Most of the above methods have problems, such as complex models and time-consuming and difficult to identify image errors. Therefore, an image identification and error correction method for test report based on DRL and the IoT platform in the smart laboratory is proposed. Through the deep learning network, the image identification is carried out, and the environment is interacted. Errors in images are identified based on reinforcement learning, so as to achieve an accurate early warning of abnormal images.

### **3. BUILDING A SMART LABORATORY BASED ON THE IOT PLATFORM**

The IoT achieves device identification, monitoring, and positioning by connecting intelligent devices to the internet. At the same time, the IoT can achieve refined management of production and life, improve resource utilization and living standards, and attain the goal of intelligence (Shapla et al., 2022). The term 'things' in the IoT mainly refers to objects that can be connected, have information transmission and processing capabilities, and are uniquely identifiable. In practical applications, communication protocols of the IoT must be strictly followed. Based on the IoT platform, a smart laboratory has been constructed, and its architecture is shown in Figure 1. According to the interface

specifications of the standard laboratory, various instruments and equipment, calibration devices, environmental sensing devices, office auxiliary devices, and mobile devices are connected downwards to achieve data collection and processing, and up to various applications on the smart laboratory platform, realizing laboratory data aggregation and uploading.

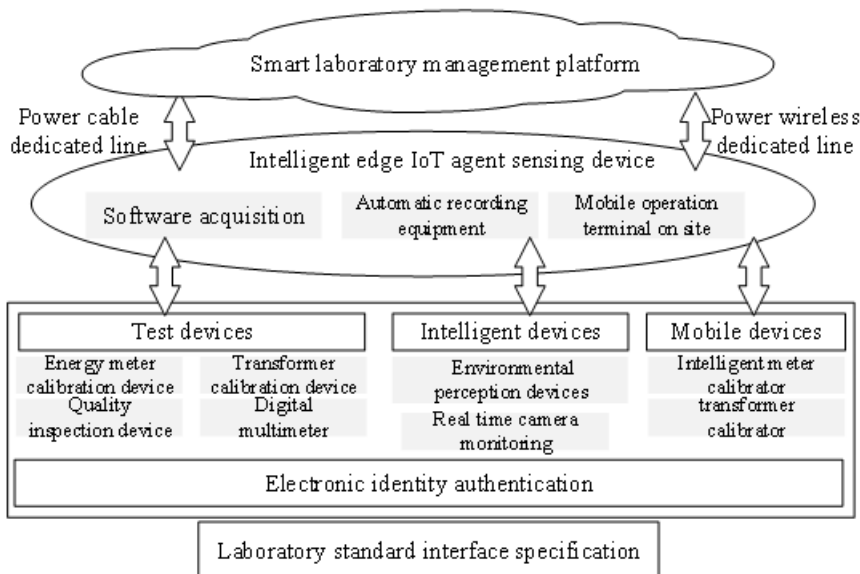
In a smart laboratory, the interconnecting equipment includes experimental equipment, intelligent equipment, and on-site equipment. The test equipment includes electric energy verification device, transformer verification device, quality inspection verification device, digital multimeter and other metering devices. Intelligent devices include various devices, such as environmental perception devices, personnel perception devices, file scanners, etc. The on-site equipment includes intelligent calibration instruments for electricity meters, intelligent calibration instruments for transformers, and other measuring instruments. The information collected by the device is uploaded to the intelligent edge agent perception device through wired or wireless means, and the information recognition is achieved through the deployed deep learning network. At the same time, by integrating environmental parameters, fault alarms, and other information, the processing results of the intelligent edge agent perception device are uploaded to the smart laboratory management platform through channels, such as the power wired private network and the power wireless private network (Xin et al., 2022). The intelligent laboratory management platform uses the deployed DRL model for information identification and error correction and distributes information such as executive feedback and warning processing to various equipment or platform software in the laboratory (Carlos Ankora, & Aju D., 2022).

#### 4. IMAGE RECOGNITION METHOD BASED ON DEEP LEARNING

##### 4.1 Image Feature Extraction Based on Improved Convolutional Neural Network

The deep information features of laboratory test report images need to be extracted through multi-layer convolutional networks, and the application of deep network structures will result in a larger model. However, in smart laboratories, the image recognition technology is set in embedded devices, and an excessively large model will increase application costs and complexity (Jason et al., 2022). Therefore,

Figure 1. Architecture of a smart laboratory



the proposed method uses deep separable convolution (DSC) to replace the multi-layer convolution layer in the convolutional neural network to obtain an improved convolutional neural network (ICNN) to reduce model complexity while improving the identification efficiency and application effectiveness of the model with lightweight features. DSC refines the standard convolution operation into depth class and point-by-point class convolutions. The internal structure of convolution is shown in Figure 2, which can reduce the number of parameters and operations in the convolution link.

When performing the standard convolution, if the size of the report information feature  $\tau$  in the input test report image is  $(C_\tau \times C_\tau \times N)$  and a convolution kernel  $\kappa$  with size  $(C_\kappa, C_\kappa, N, M)$  is introduced for convolution, the output feature  $\xi$  size is  $(C_\xi \times C_\xi \times M)$ , where  $C_\tau$  and  $C_\kappa$  are the width and the height of the test report information feature and the convolution kernel;  $N, M$  is the number of input and output channels. Through DSC,  $\xi$  can be mapped to  $\tau$ , and a hyperparameter  $v$  can be imported to control the input and output channel quantities. The computational complexity is calculated as follows:

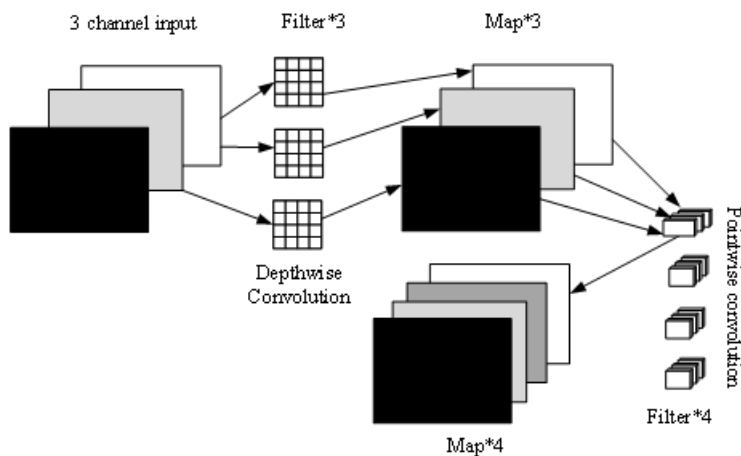
$$\frac{C_\kappa \times C_\kappa \times vN \times C_\tau \times C_\tau + vN \times vM \times C_\tau \times C_\tau}{C_\kappa \times C_\kappa \times N \times M \times C_\tau \times C_\tau} = \frac{v}{M} + \frac{v}{C_\kappa^2} \quad (1)$$

After obtaining the feature map of test report information through ICNN feature serialization, feature vectors are extracted from the pixel values of each column of the feature map from left to right. In this operation, each column of the test report information feature vector corresponds to a rectangular range in the feature map.

#### 4.2 Image Recognition Based on Bidirectional Recurrent Network

Due to the effective utilization of input forward and backward feature information and the ability to learn long-term dependencies between features, the proposed method inputs the test report image features extracted by ICNN into the bidirectional recurrent network for analysis; thereby, obtaining reliable image recognition results. A forward recurrent neural network and a backward recurrent neural network are combined to form a bidirectional recurrent neural network, and the network is updated through the back propagation mode. Since the long short memory network (LSTM) can avoid the vanishing gradient problem in the traditional recurrent neural model, BiLSTM is selected for image

Figure 2. Internal structure of DSC convolution



recognition, and the full connection layer is introduced behind the bidirectional recurrent neural networks. To avoid the overfitting problem, a dropout layer is added inside the BiLSTM structure, and the identification results of the experimental test report image are output through the Softmax classification function. The overall structure of the image recognition model is shown in Figure 3.

The forward and backward LSTM structures in BiLSTM are the same, but do not share parameters. The input sequence is obtained by a dimensionality reduction of the feature matrix extracted from the ICNN layer, represented by  $X = \{x_1, x_2, \dots, x_t, \dots, x_T\}$ . When processing input data  $X$  at time  $t$ , the forward and reverse LSTM hidden layers are  $\vec{h}_t$  and  $\overleftarrow{h}_t$ . The updating is as follows:

$$\begin{aligned} \vec{h}_t &= \varphi' \left( \omega_{x \vec{h}} x_t + \omega_{\vec{h} \vec{h}} \vec{h}_{t-1} + b_{\vec{h}} \right) \\ \overleftarrow{h}_t &= \varphi \left( \omega_{x \overleftarrow{h}} x_t + \omega_{\overleftarrow{h} \overleftarrow{h}} \overleftarrow{h}_{t-1} + b_{\overleftarrow{h}} \right) \end{aligned} \quad (2)$$

Where  $\omega$  is the weight parameter;  $b$  is offset;  $\varphi$  and  $\varphi'$  represents forward and backward operation operations.

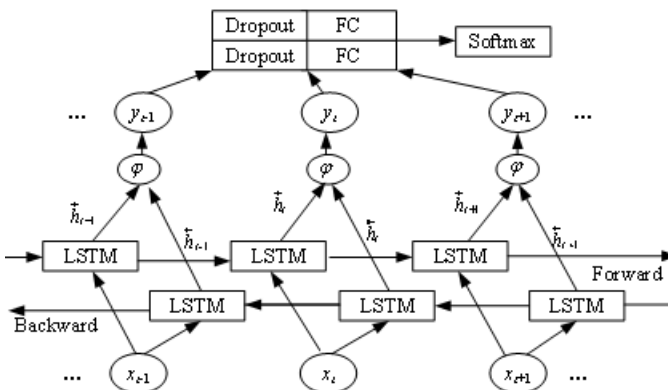
In addition, after adding the dropout layer to BiLSTM, the calculation of the fully connected layer is as follows:

$$c = \sigma \left( \omega_h H \Theta(p) + b_h \right) \quad (3)$$

Where  $\Theta(p)$  is the probability vector generated, randomly deleting neurons with a  $p$ -ratio to prevent overfitting;  $\sigma$  is the activation function;  $H$  is the output of the hidden layer.

After the test report image features are processed by BiLSTM, a high-performance classifier needs to be added to classify the input image categories. The proposed method uses a Softmax classifier, and the classifier based on the Softmax function output layer calculates a probability for each image category (Min & Sheng, 2023). Assuming that the probability of sample  $x$  belonging to the  $i$ -th category is  $p(y = i | x, \vartheta)$ , then the loss function  $J(\vartheta)$  based on log maximum likelihood function for training classifier is calculated as follows:

Figure 3. Overall structure of the image recognition model



$$J(\vartheta) = -\sum_{i=1}^{\Omega} \log\left(p\left(y = y^{(i)} \mid x^{(i)}, \vartheta\right)\right) \quad (4)$$

Where  $\vartheta$  is the model parameter;  $\Omega$  represents the training set;  $\left(x^{(i)}, y^{(i)}\right)$  is the  $i$ -th training sample.

The output gate of the BiLSTM neural network can calculate the image category label corresponding to the input through the activation function and measure the input image label and the network output result to calculate the loss function. If the difference between the output category and the input image tag is small, the loss function value is small, and the training process of the BiLSTM network is the process of reducing the loss function value through continuous iterations. Subsequently, the output feature vectors are fed into the Softmax classifier for processing. In multi-classification tasks, the output of the network is the score for each class corresponding to the input image. Through the Softmax classifier, the predicted probability value for the corresponding class of the input image can be obtained; thereby achieving image recognition.

## 5. ERROR CORRECTION METHOD OF TEST REPORT BASED ON DRL

### 5.1 DRL

Reinforcement learning mainly seeks the optimal strategy by constant exploring attempts, that is, agents gradually learn to control behavior through self-exploration of the environment. The reinforcement learning problem is often modeled by Markov Decision Process (MDP). MDP can be expressed as a three tuple  $\{S, A, R\}$ :  $S$  represents the state space,  $A$  represents the action space, and  $R$  represents the reward (Liman & Yen, 2022). DRL is a new algorithm developed by Google's DeepMind artificial intelligence research team by combining the deep network with intelligent perception ability and reinforcement learning with intelligent decision-making ability (Çağrı et al., 2023).

Q-learning algorithm is one of the important algorithms in reinforcement learning. In the process of reinforcement learning, agents interact with the environment (that is, state space), and use rewards as guidance to enable agents to obtain the most rewards, thus obtaining the optimal diagnosis strategy. When selecting the corresponding action during the interaction process, the Q value is used to evaluate its value. The Q value represents the expected total reward that the agent can receive in the final state after selecting an action. When the number of states and actions is limited, traditional Q-learning algorithms can determine actions by looking up Q-tables; however, when dealing with a large number of states and actions, mapping the relationship between actions and states using a table method may lead to a curse of dimensionality. Therefore, a deep neural network is used to fit an optimal Q function, namely a DQN, to solve this problem.

In DQN, a state action value function  $Q(s_t, a_t)$  is defined, and the Q value of the agent when selecting action  $a_t$  using the optimal strategy  $\pi$  in state  $s_t$  is calculated as follows:

$$\pi(s_t) = \arg \max_{a_t} Q(s_t, a_t) \quad (5)$$

The optimal function  $\hat{Q}(s_t, a_t)$  is defined to represent the highest cumulative reward value obtained by the intelligent agent when taking action  $a_t$  in state  $s_t$ . The formula follows the Bellman equation, and  $\hat{Q}(s_t, a_t)$  is calculated as follows:

$$\hat{Q}(s_t, a_t) = E \left[ r_t + \gamma \max_{a_{t+1}} Q(s_{t+1}, a_{t+1}) \right] \quad (6)$$

Where  $\gamma$  is the discount factor,  $s_{t+1}$  is the next state, and  $a_{t+1}$  is the action selected based on the optimal strategy  $\pi$ . After value iterations are repeated,  $Q(s_t, a_t)$  converges to  $\hat{Q}(s_t, a_t)$ .

When the depth neural network is used to fit the Q function, the Q function is approximately  $Q(s_t, a_t; \theta)$  from the depth neural network with the weight of  $\theta$ , and its loss function is defined as follows:

$$L(\theta) = (y - Q(s_t, a_t; \theta))^2$$

$$y = \begin{cases} r_t, s_{t+1} \text{ is terminal} \\ r_t + \gamma \max_{a_{t+1}} Q(s_{t+1}, a_{t+1}; \hat{\theta}), \text{ otherwise} \end{cases} \quad (7)$$

Where  $y$  is the target value,  $\hat{\theta}$  is the parameter of the target network, and the structure of the target network is the same as the current network  $Q(s_t, a_t; \theta)$ .

The proposed method uses the experience playback to stabilize the convergence process and constructs an experience pool  $P$  to store the state transition records of agents, where the state transition records of agents are obtained using the  $\epsilon$ -greedy strategy, and then we extract the experience samples stored in  $P$  and train the Q network by minimizing the loss function. The gradient descent is used to update the Q network parameters  $\theta$  iteratively, and the interaction process in the environment is continuously simulated, and new state transition records are stored to replace the old transition records. Until the target network has merged with the current network, the training process repeats itself. The update calculation for  $\theta$  is as follows:

$$\theta = \hat{\theta} + \epsilon \frac{\nabla L(\theta)}{\nabla \theta}$$

$$= \hat{\theta} + \epsilon \left[ -2(y - Q(s_t, a_t; \theta)) \frac{\nabla Q(s_t, a_t; \theta)}{\nabla \theta} \right] \quad (8)$$

Where  $\epsilon$  is the learning rate.

After each optimization, the parameter  $\hat{\theta}$  of the target network is updated as follows:

$$\hat{\theta} = \theta + \lambda \nabla Q(s_t, a_t; \theta) \quad (9)$$

Where  $\lambda$  is the update factor of the target network.

## 5.2 Multi-Head Attention Model

ICNN and BiLSTM networks are used as agents of the reinforcement learning model to identify and correct test report images. The process is shown in Figure 4. It mainly includes three steps: (1) Test report image feature extraction CNN part; (2) Image feature sequence analysis LSTM part; (3) Identification and error correction action decision-making part.

Figure 4. Test report error correction process based on DRL

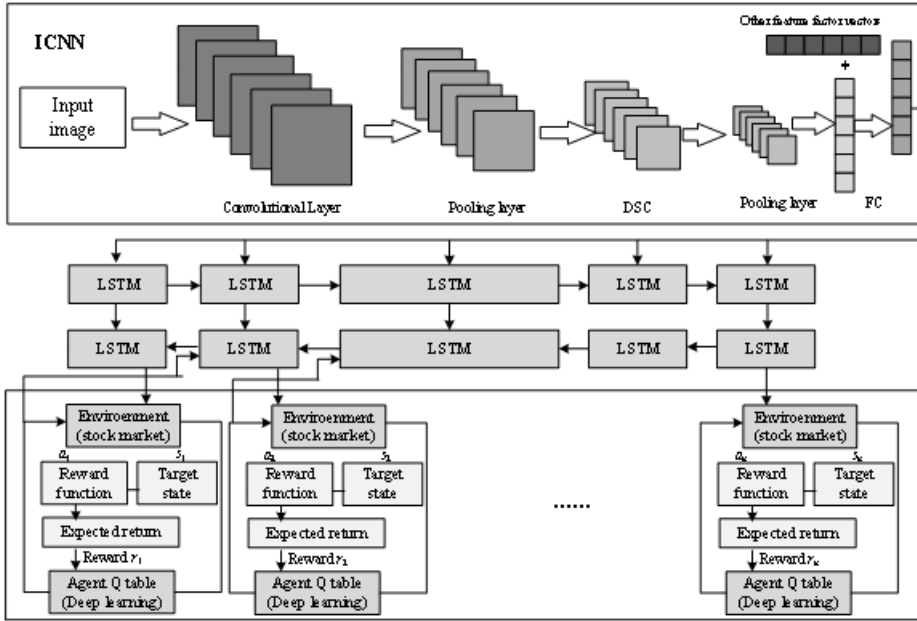


Image  $X_u$  is the image input and it is currently observed by the intelligent agent and the reference standard image  $X_0$ . After extracting features through ICNN, it is input into the BiLSTM network, and the strategy  $\pi(s_t; \theta)$  and value  $V(s_t; \theta_v)$  are outputs by two fully connected layers (FC). When the intelligent agent performs an image recognition action according to  $\pi(s_t; \theta)$ , it will receive the reward  $R_t$  and state  $S_t$  returned by the intelligent laboratory, as well as the pre-sequence  $h_t$  processed by BiLSTM as the input for the next neuron,  $h_{t+1} = LSTM(a_t, c_{out}, h_t)$ , where  $c_{out}$  is the external input image signal, the intelligent agent action can be rewritten as  $a_t = \phi^0(h_t, s_t)$ , and the Q function can be rewritten as  $Q^0(h_{t+1}^i, \phi^0(h_{t+1}^i, s_{t+1}))$ .

The updated network loss function is:

$$L(\theta) = E \left[ \left( y_t - Q^0 \left( h_{t+1}^i, \phi^0 \left( h_{t+1}^i, s_{t+1} \right) \right) \right)^2 \right] \quad (10)$$

$$y_t = r + \gamma Q^0 \left( h_{t+1}^i, \phi^0 \left( h_{t+1}^i, s_{t+1} \right) \right)$$

Equation (10) is solved to minimize the loss function, where  $h_{t+1}^i$  is the BiLSTM output at time  $t + 1$ ,  $s_{t+1}$  is the environmental state at time  $t + 1$ , and  $\theta_i$  and  $\hat{\theta}_i$  are the training process parameters and target network parameters of the value function Q, and  $\hat{\theta}_i$  is updated intermittently during the training process.

Within each part of the intelligent agent network, ICNN is used to extract image features, obtain state features of each time step, and interact with the environment in turns to obtain a sequence of state features, which are input into the BiLSTM network for image recognition. During the image

recognition, when the environment interacts with  $a_t$ , intelligent agents use  $V(s_t; \theta_v)$  to solve the current state value  $v$  and use it as a standard to measure the current  $X_u$  and  $X_0$  states. The Euclidean distance  $D$  of key points in  $X_u$  and  $X_0$  is simultaneously used for error correction, and if  $D$  is less than the set threshold, it indicates that the test report image is correct; on the contrary, if there are errors in the test report image, an alert will be issued.

## 6. EXPERIMENTS AND ANALYSIS

### 6.1 Experimental Environment

In the experiment, Python 3.4 was used to implement the algorithm model, and Tensorflow function module was used to develop a deep learning network. Use Python matplotlib 3.1 library to realize data and information visualization, with 64 GB of memory, CPU i7 4790, GPU GTX1070, and CUDA 9.0 and CUDNN 7.1 to speed up the calculation (Markiewicz & Koperwas, 2022).

Parameters for the DRL network are set as follows: CNN filter is  $3 \times 3$ , quantity is 32, step size is 1, and pool size is  $2 \times 2$ . Dropout is set to 0.5. The input size of BiLSTM is 24, and the number of units of each layer is 128. The activation function used is ReLU, Epochs=50. The Bellman discount factor is 0.9, the experience playback pool size is set to 100,000, the greedy strategy is 0.9, and the termination value is 0.001. During the training process, the off policy method is used, and the target network is updated every 100 steps.

In addition, accuracy and error rates were used for indicator evaluation in the experiment, and the average execution time of different methods in the same number of executions (set to 10) was used as the processing time.

### 6.2 Determination of Model Parameters

In the experiment, when testing the performance of the ICNN model, the convolution kernel size has a significant impact, and a reasonable convolution kernel size needs to be set. We set the convolution kernel size to  $2 \times 2$ ,  $4 \times 4$ ,  $6 \times 6$  in sequence. The accuracy and efficiency of image recognition are shown in Table 1.

From Table 1, it can be seen that as the number of images increases in sequence, the identification accuracy of the proposed method is consistent under the same convolutional kernel size. However, the larger the convolutional kernel, the higher the identification accuracy. When the convolutional kernel size is  $6 \times 6$ , the identification accuracy reaches 99.54%. However, due to the large convolutional kernel, the number of training parameters will also increase, resulting in slower network training speed and longer convergence time. As a result, image recognition takes more time and efficiency

Table 1. Influence of convolutional kernel size on identification performance

Index	Number of images/ frame	Convolutional kernel size		
		$2 \times 2$	$4 \times 4$	$6 \times 6$
Time/s	100	1.22	1.22	1.25
	200	1.24	1.25	1.27
	300	1.27	1.28	1.31
	400	1.30	1.30	1.36
	500	1.34	1.35	1.40
Accuracy/%	100-500	97.15	98.37	99.54

decreases. When the convolutional kernel size is  $6 \times 6$ , its maximum identification time reaches 1.40s. Therefore, considering the recognition effect comprehensively, the optimal value of convolutional kernel size is set to  $4 \times 4$ . At this point, the proposed method has an image recognition accuracy of up to 98.37%, and the recognition time is lower than that of the convolutional kernel size of  $6 \times 6$ , which is close to the recognition time of the convolutional kernel size of  $2 \times 2$ , but the recognition accuracy is significantly improved.

At the same time, the setting of different learning rates in the DRL model is also crucial. The performance of the proposed method under different learning rates is analyzed through the loss function curve. The experimental results are shown in Figure 5.

As shown in Figure 5, with the increase of learning rate, the convergence rate of the loss function value is accelerated. At the same time, with the continuous increase of training times, the loss function under different learning rates showed a downward trend. After 150 times of training, the decrease of loss function value slowed down; when the number of training reaches 250, the curve begins to stabilize, and when the learning rate is  $10^{-3}$ , the loss function value is the lowest, lower than 10. Therefore, when the learning rate is  $10^{-3}$ , the proposed method has the best performance.

### 6.3 Analysis of Image Recognition Results

#### 6.3.1 Performance Analysis of Deep Learning Models

In order to demonstrate the performance of the deep neural network in the DRL model, the basic CNN is compared with ICNN and ICNN-BiLSTM. Among them, ICNN is an improved model of CNN, while ICNN-BiLSTM is a deepened application of ICNN model. They have comparability. 1,000 test report images are selected in the experiment, and the identification accuracy of the three models is shown in Figure 6.

From Figure 6, CNN tends to converge after about 100 times, and the final training accuracy is less than 90%, while ICNN uses DSC to reduce the number of parameters and operations in the convolution link; thus, accelerating the convergence rate. When the number of iterations reach 80, the ICNN model tends to converge and the training accuracy exceeds 90%. Owing to the proposed ICNN-BiLSTM model, which extracts features from ICNN and introduces BiLSTM model to learn

Figure 5. Loss function curve under different learning rates

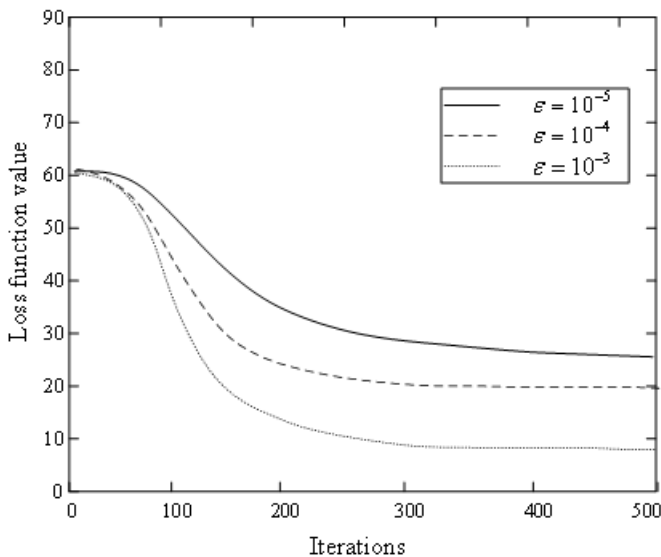
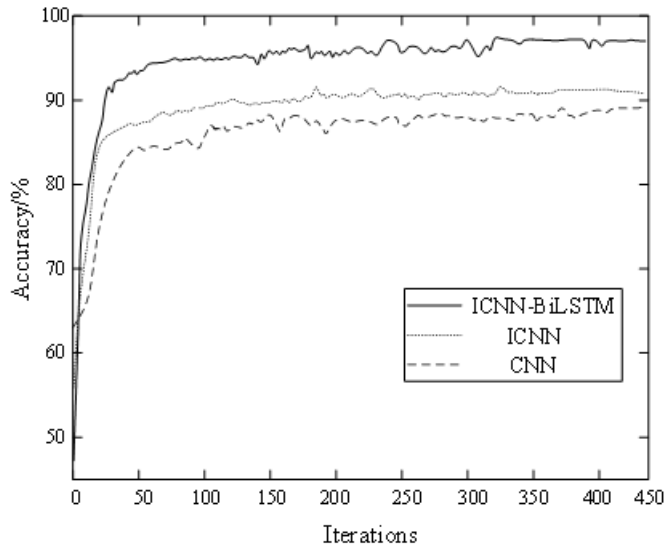


Figure 6. Performance curve of ICNN-BiLSTM comparative model



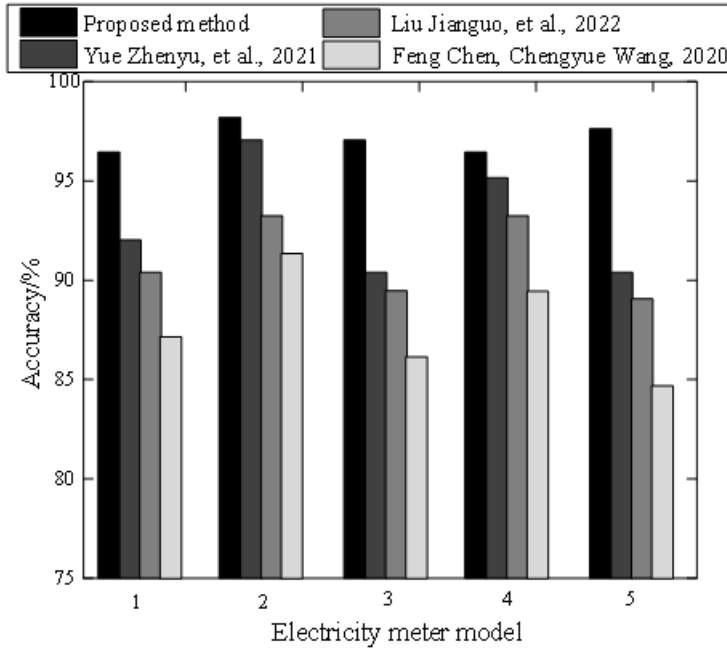
and classify image features, the training accuracy is improved by up to 96.75%. At the same time, the dropout layer is added to the BiLSTM model, which can accelerate the convergence rate of the model. When the number of iterations is 50, the ICNN-BiLSTM model tends to be stable.

### 6.3.2 Analysis of Image Recognition Results for Test Report

Taking smart meters as an example, a total of 1,000 meters of five models are selected for inspection and testing in the smart laboratory. 1,000 test report images are input into the proposed method and identified in Chen and Wang (2020), Jianguo et al. (2022), and Zhenyu et al. (2021). The identification accuracy is shown in Figure 7. Among them, Chen and Wang (2020) adopt a traditional method, Jianguo et al. (2022) and Zhenyu et al. (2021) both use deep learning methods, but Jianguo et al. (2022) proposes a single model. Zhenyu et al. (2021) on the other hand, uses a fusion model, and all three methods are representative.

From Figure 7, it can be seen that the proposed method can achieve an identification accuracy of about 96% for the image recognition of five types of electricity meter test reports, and the fluctuations are not significant, indicating a certain degree of identification stability. Because of the combination of ICNN and BiLSTM models in the proposed method, reliable features extracted by ICNN are input into the BiLSTM model for learning, effectively ensuring identification accuracy. At the same time, the ICNN-BiLSTM model has strong identification ability and can recognize various images in different environments. Chen and Wang (2020) used binarization to obtain image features and Bayesian classifier to achieve intelligent recognition. This method has a simple structure and weak feature extraction ability, resulting in an identification accuracy of about 87%. Moreover, the identification results of different types of electricity meters fluctuate significantly. Jianguo et al. (2022) utilized ASGS-CWOA to optimize the parameters of the BP neural network, and also applied it for image recognition. The performance of this method has been improved to some extent compared to Chen and Wang (2020), but for image recognition in complex backgrounds, its accuracy needs to be improved, such as for meter type 5, whose identification accuracy is less than 90%. Zhenyu et al. (2021) used ACNN to extract image features and FMC to calculate the similarity score between the feature map and the prototype, thus completing image recognition. This method combines ACNN and FMC models to achieve high identification accuracy. For example, for meter 2 with a relatively

Figure 7. Comparison of identification results of different models



simple test report image, its identification accuracy exceeds 95%, close to the proposed method. However, for complex images, its recognition performance needs further improvement.

## 6.4 Analysis of Image Error Correction Results for Test Report

### 6.4.1 Performance Analysis of DRL Model

In the experiment, 500 smart meter test reports were randomly selected from the total sample, of which 490 were normal reports and 10 were error reports. A total of 50 rounds are set for the training model process, and 64 steps are set for each round of training process. The DRL network is trained according to the reward value updating method and network iteration process described above. The accuracy rate and loss function of the trained network model are shown in Figure 8.

As seen in Figure 8, with the increase of training rounds, the error correction accuracy of the proposed DRL model is gradually increasing. After 17 rounds of training, the model stabilized, with an error correction accuracy of about 95%, and the loss value gradually stabilized at around 0.001. It can be argued that the proposed model is effective for identifying and correcting test report images.

### 6.4.2 Comparison of Error Correction Results Using Different Methods

In order to demonstrate the comprehensive performance of the proposed method, it was compared with the error correction encoding method, deep Q-network (DQN), and methods in Lifeng et al. (2022). The image error correction error is shown in Figure 9.

In Figure 9, it can be seen that compared with other methods, the error correction error of the proposed method is the smallest, only about 4%. As it uses ICNN-BiLSTM as an agent to interact with the environment, the test report with errors is obtained through reinforcement learning. Due to the lack of high-performance intelligent agents, the error correction error of traditional DQN has been improved, reaching around 8%. Lifeng et al. (2022) combined DenseNet and DPRN models for image recognition and anomalies are identified, but there is a lack of interactive learning with the environment, resulting in large fluctuations in error correction errors, approaching 10%. The

Figure 8. Training curve of DRL model

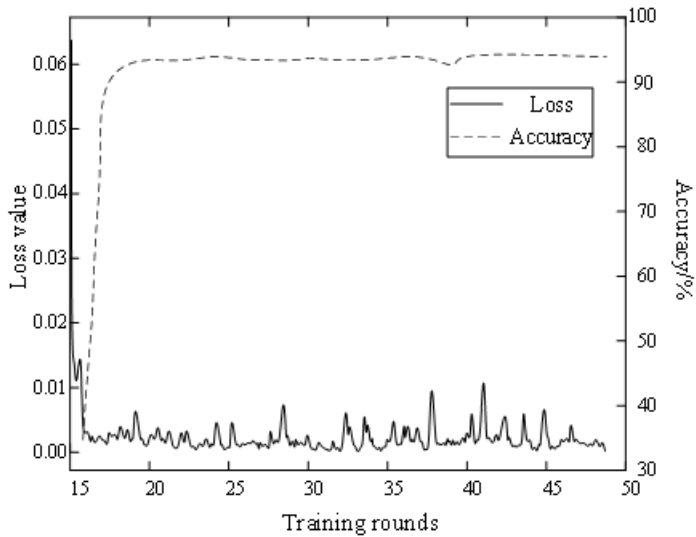
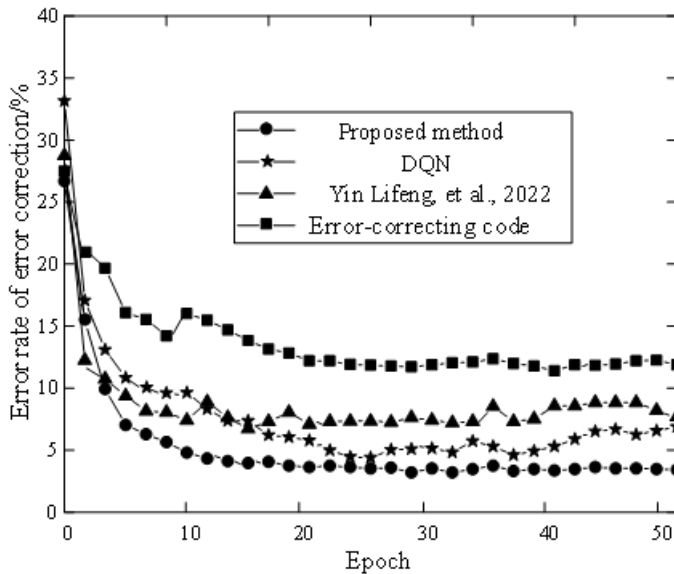


Figure 9. Comparison of correction errors for image error using different methods



conventional error correction coding method has significant limitations in its application and lacks reliable feature extraction capabilities, resulting in the largest error correction error of about 12%. Thus, it can be seen that the proposed method has obvious advantages in image error correction.

Common errors in test report images include data errors (A), image skewing (B), non-standard unit symbols (C), and table misalignment (D). 440 test reports with errors were selected and analyzed using the proposed method and deep Q network (DQN). The error correction accuracy and processing time are shown in Table 2.

**Table 2. Comparison of error correction accuracy and processing time of different methods**

Method		DQN	Proposed method
Accuracy/%	A/150	90.28	94.37
	B/120	92.53	97.41
	C/90	91.78	96.08
	D/80	93.04	99.15
Mean accuracy/%		91.91	96.75
Time/s		13.89	15.37

As seen in Table 2, two kinds of DRL networks are used to identify and correct the error sample images in the test set, and the proposed method has a high error correction accuracy rate for all kinds of error reports, with the average accuracy rate reaching 96.75%, especially for the detection of image tilt and table dislocation, where the accuracy rate exceeds 97%. This is because compared to the DQN network, the proposed method selects ICNN-BiLSTM as the intelligent agent, which has better image extraction and recognition capabilities and can improve the error correction accuracy. However, the more complex structure also leads to an increase in error correction time. The processing time of the proposed method is 15.37s, which is 1.48s longer than DQN. Overall, applying the proposed method to identify and correct test report images in smart laboratories can achieve outstanding results.

## 7. CONCLUSION

For a better adaptation to the intelligent upgrading of power grid business and in order to achieve efficient processing of smart laboratory test reports, an image recognition and error correction method for test reports based on DRL and the IoT platform is proposed. On the smart laboratory platform, the ICNN-BiLSTM model is used for precise image recognition, and it is also used as an intelligent agent for reinforcement learning models. By calculating the distance between the key points of the identified image and the reference image, the reliable error correction of the image is determined. The experimental results based on the Python platform indicate that:

- 1) ICNN - BiLSTM model has reliable image identification performance, which can achieve an identification accuracy of about 96%, and the fluctuation is not obvious in different environments. At the same time, with the help of DSC operation, its convergence rate is also high.
- 2) The proposed method utilizes the ICNN-BiLSTM model as an intelligent agent for interactive learning, which can accurately identify error reports. Its average error correction accuracy reaches 96.75%, and the processing time is 15.37s, which is superior to other comparative methods.

The basic logic of DRL network is similar to that of human thinking, representing the most possible development direction of automation. In future research, the migration algorithm will be introduced into DRL to solve the scarcity problem of effective data in the real laboratory.

## AUTHOR CONTRIBUTIONS

XiaoJun Li and PeiDong He performed the project administration; WenQi Shen and KeLi Liu performed the formal analysis; ShuYu Deng performed the data curation; Li Xiao wrote the original draft.

## **FUNDING INFORMATION**

This work was supported by the State Grid Sichuan Electric Power Corporation (52199722000A), “Research on digital confirmation method technology of standard equipment traceability result.”

## **CONFLICTS OF INTEREST**

The authors declare no conflicts of interest.

## **DATA AVAILABILITY STATEMENT**

The original data can be obtained by contacting the corresponding author.

## REFERENCES

- Ankora, C., & D, A. (2022). Integrating user stories in the design of augmented reality application. [IJITSA]. *International Journal of Information Technologies and Systems Approach*, 15(1), 1–19. doi:10.4018/IJITSA.304809
- Çağrı, K., Ayşegül, U., & Cüneyt, G. (2023). Development of a new robust stable walking algorithm for a humanoid robot using deep reinforcement learning with multi-sensor data fusion. *Electronics (Basel)*, 12(3), 568. doi:10.3390/electronics12030568
- Chavarkar, S. (2023). A review of deep learning models for wireless sensor networks. *Journal of Research in Science and Engineering*, 5(1), 1.
- Chen, F., & Wang, C. (2020). Image recognition technology based on cloud computing platform. *Journal of Intelligent & Fuzzy Systems*, 39(4), 1–11. doi:10.3233/JIFS-179997
- Dongxing, W., Jingxiu, N., & Tingyu, D. (2022). An image recognition method for coal gangue based on ASGS-CWOA and BP neural network. *Symmetry*, 14(5), 880. doi:10.3390/sym14050880
- Ersheng, P., Siwei, L., Jianqin, L., Qingru, Q., & Zun, G. (2020). The state grid corporation of China's practice and outlook for promoting new energy development. *Energy Conversion and Economics*, 1(2), 71–80. doi:10.1049/enc2.12007
- Fernandes, S. S., Astuto, A., Patrão, K. C. S., Fonseca, E. S., Pereira, W. W., & Lopes, R. T. (2018). Experimental and computational evaluation of effective centre from a long counter at neutron metrology laboratory in Brazil. *Radiation Protection Dosimetry*, 180(1-4), 37–41. doi:10.1093/rpd/ncy080 PMID:29788424
- Giacomo, P., Alessandro, P., & Mattia, V. D. M. (2023). Fight fire with fire: Detecting forest fires with embedded machine learning models dealing with audio and images on low power IoT devices. *Sensors (Basel)*, 23(2), 783. doi:10.3390/s23020783 PMID:36679579
- Guoming, C., & Qinghua, L. (2022). Overview of ship image recognition methods based on computer vision. *Journal of Physics: Conference Series*, 2387(1), 1.
- Jason, B., Zahra, G., & Nawin, R. (2022). CNN based image classification of malicious UAVs. *Applied Sciences (Basel, Switzerland)*, 13(1), 240. doi:10.3390/app13010240
- Jianguo, L., Kai, J., & Yan, J. (2022). Image recognition and extraction of students' human motion features based on graph neural network. *Computational Intelligence and Neuroscience*, 2022, 6755053. PMID:35371232
- Lifeng, Y., Pujiang, H., Guanghai, Z., Huayue, C., & Wu, D. (2022). A novel image recognition method based on DenseNet and DPRN. *Applied Sciences (Basel, Switzerland)*, 12(9), 4232. doi:10.3390/app12094232
- Liman, J., & Yen, L. H. (2022). Reinforcement learning for channel and radio allocations to wireless backhaul links. *IEICE Proceeding Series*, 70, PS3-09.
- Lu, H., Qingying, L., Weichen, P., Rao, Y., & Senyun, L. (2022). Ice accretion thickness prediction using flash infrared thermal imaging and BP neural networks. *IET Image Processing*, 17(3), 649–659.
- Markiewicz, M., & Koperwas, J. (2022). Evaluation platform for DDM algorithms with the usage of non-uniform data distribution strategies. [IJITSA]. *International Journal of Information Technologies and Systems Approach*, 15(1), 1–23. doi:10.4018/IJITSA.290000
- Masayuki, O., Takumi, O., Tetsushi, K., Toru T., Shigeto Y., Hiroshi M., Shinji T., (2022). Classification with CNN features and SVM on Embedded DSP Core for Colorectal Magnified NBI Endoscopic Video Image. *IEICE Transactions on Fundamentals of Electronics, Communications and Computer Sciences*, E105.A(1), 25-34.
- Min, Z. J., & Sheng, L. Q. (2023). Multi-centers SoftMax reciprocal average precision loss for deep metric learning. *Neural Computing & Applications*, 35(16), 11989–11999. doi:10.1007/s00521-023-08334-1
- Najib, U., Ismail, M. M., Kifayat, U., Mohammed, S. M. G., Liaqat, A., Shafqat Ullah, K., & Niamat, U. (2022). Diabetic retinopathy detection using genetic algorithm-based CNN features and error correction output code SVM framework classification model. *Wireless Communications and Mobile Computing*, 2022, 1.

Sardjono, R. H. (2021). Simplification of null method measurement system to build a standalone DC voltage standard traceability system in the SNSU - BSN electrical metrology laboratory. *Journal of Physics: Conference Series*, 1816(1), 012011–012023. doi:10.1088/1742-6596/1816/1/012011

Shapla, K., Ismail, A., Idna, I. M. Y., & Mohamed, H. J. (2022). Towards an effective intrusion detection model using focal loss variational autoencoder for Internet of Things (IoT). *Sensors (Basel)*, 22(15), 5822. doi:10.3390/s22155822 PMID:35957379

Shintaro, O., Kazunori, N., & Mikako, H. (2023). An efficient annotation method for image recognition of dental instruments. *Scientific Reports*, 13(1), 169. doi:10.1038/s41598-022-26372-y PMID:36599858

Song, Y. (2021). Traffic sign recognition based on HOG feature extraction. *Journal of Measurements in Engineering*, 9(3), 142–155. doi:10.21595/jme.2021.22022

Xin, L., Cun, Z. D., Yang, H. L., & Ti, W. D. (2022). Hybrid air route network simulation based on improved RW-bucket algorithm. [IJITSA]. *International Journal of Information Technologies and Systems Approach*, 15(1), 1–19. doi:10.4018/IJITSA.304808

Xinrong, Y., Zhengping, L., & Chao, X. (2022). Ghost-free multi-exposure image fusion technology based on the multi-scale block LBP operator. *Electronics (Basel)*, 11(19), 3129. doi:10.3390/electronics11193129

Zhenyu, Y., Fei, G., Qingxu, X., Jinping, S., Amir, H., & Huiyu, Z. (2021). A novel few-shot learning method for synthetic aperture radar image recognition. *Neurocomputing*, 465, 215–227. doi:10.1016/j.neucom.2021.09.009

Zhiyu, G., Bailin, L., Hongxian, G., & Jing, M. (2020). Research on the application of convolutional neural networks in the image recognition. *International Journal of Advanced Network. Monitoring and Controls*, 5(2), 31–38. doi:10.21307/ijanmc-2020-014

*XiaoJun Li received his master's degree in control science and engineering from Tsinghua University. He is currently a senior engineer of State Grid Sichuan Electric Power Corporation Metering Center. His research interests include electrical measurement technology, carbon metering, the new power system, machine vision inspection systems, and image processing.*

*PeiDong He received his master's degree in electrical engineering from the School of Electrical Engineering of Chongqing University. He is currently a senior expert of State Grid Sichuan Electric Power Company. His research interests include carbon metering, electrical measurement technology, and measurement data fusion application.*

*WenQi Shen received her master's degree in instrumentation engineering from University of Electronic Science and Technology of China. She is currently a senior engineer of State Grid Sichuan Electric Power Corporation Metering Center. Her research interests include electrical measurement technology and the new power system.*

*KeLi Liu received his bachelor's degree in electrical engineering and automation from Sichuan University. He is currently a senior engineer of State Grid Sichuan Electric Power Corporation Metering Center. His research interests include electrical measurement technology and electrical energy standard and device testing systems.*

*ShuYu Deng received his master's degree in instrument science and technology from Harbin Institute of Technology. He is currently a senior engineer of State Grid Sichuan Electric Power Corporation Metering Center. His research interests include electrical measurement technology, the new power system, and time-frequency measurement.*

*LI Xiao is currently an engineer of State Grid Sichuan Electric Power Corporation Metering Center. Her research interests include electrical measurement technology, the new power system, and image processing.*